


ORIGINAL RESEARCH

Open Access

# Renal $^{99m}\text{Tc}$ -DMSA pharmacokinetics in pediatric patients



Donika Plyku<sup>1</sup>, Michael Ghaly<sup>1</sup>, Ye Li<sup>1</sup>, Justin L. Brown<sup>2</sup>, Shannon O'Reilly<sup>2</sup>, Kitiwat Khamwan<sup>1,3</sup>, Alison B. Goodkind<sup>4</sup>, Briana Sexton-Stallone<sup>4</sup>, Xinhua Cao<sup>4</sup>, David Zurakowski<sup>5</sup>, Frederic H. Fahey<sup>4</sup>, S. Ted Treves<sup>6</sup>, Wesley E. Bolch<sup>2</sup>, Eric C. Frey<sup>1</sup> and George Sgouros<sup>1\*</sup> 

\* Correspondence: [gsgouros@jhmi.edu](mailto:gsgouros@jhmi.edu)

<sup>1</sup>The Russell H. Morgan Department of Radiology and Radiological Science, Johns Hopkins University, School of Medicine, Baltimore, MD, USA

Full list of author information is available at the end of the article

**Abstract:**  $^{99m}\text{Tc}$ -DMSA is one of the most commonly used pediatric nuclear medicine imaging agents. Nevertheless, there are no pharmacokinetic (PK) models for  $^{99m}\text{Tc}$ -DMSA in children, and currently available pediatric dose estimates for  $^{99m}\text{Tc}$ -DMSA use pediatric *S* values with PK data derived from adults. Furthermore, the adult PK data were collected in the mid-70's using quantification techniques and instrumentation available at the time. Using pediatric imaging data for DMSA, we have obtained kinetic parameters for DMSA that differ from those applicable to adults.

**Methods:** We obtained patient data from a retrospective re-evaluation of clinically collected pediatric SPECT images of  $^{99m}\text{Tc}$ -DMSA in 54 pediatric patients from Boston's Children Hospital (BCH), ranging in age from 1 to 16 years old. These were supplemented by prospective data from twenty-three pediatric patients (age range: 4 months to 6 years old).

**Results:** In pediatric patients, the plateau phase in fractional kidney uptake occurs at a fractional uptake value closer to 0.3 than the value of 0.5 reported by the International Commission on Radiological Protection (ICRP) for adult patients. This leads to a 27% lower time-integrated activity coefficient in pediatric patients than in adults. Over the age range examined, no age dependency in uptake fraction at the clinical imaging time was observed. Female pediatric patients had a 17% higher fractional kidney uptake at the clinical imaging time than males ( $P < 0.001$ ).

**Conclusions:** Pediatric  $^{99m}\text{Tc}$ -DMSA kinetics differ from those reported for adults and should be considered in pediatric patient dosimetry. Alternatively, the differences obtained in this study could reflect improved quantification methods and the need to re-examine DMSA kinetics in adults.

**Keywords:** DMSA, Pediatric imaging, Compartmental modeling, Pharmacokinetics, Dose reduction/optimization

### Introduction

The activity administered to pediatric nuclear medicine patients is currently based on the joint, consensus guidelines from the Society of Nuclear Medicine and Molecular Imaging (SNMMI) and the European Association of Nuclear Medicine (EANM) [1–3]. These guidelines assure consistency across different institutions while also promoting dose reduction; however, the recommended administered activities are based on a consensus approach rather than on a rigorous and quantitative approach. <sup>99m</sup>Tc-dimercaptosuccinic acid (DMSA) is one of the most commonly used pediatric nuclear medicine imaging agents. Nevertheless, there are no pharmacokinetic (PK) models for <sup>99m</sup>Tc-DMSA in children and currently available pediatric dose estimates for <sup>99m</sup>Tc-DMSA use pediatric *S* values with PK data derived from adults using instrumentation and quantification techniques dating to the mid-70’s [4–9]. We have previously demonstrated that accounting for body habitus (height and weight) and organ size differences yields greater accuracy compared with a weight-only-based model [10–13]. As part of an ongoing dose optimization effort [10, 11, 14, 15], we examine whether the current reference (ICRP 53 [4]) DMSA PK model is consistent with model parameters obtained by <sup>99m</sup>Tc-DMSA imaging quantification in children using current quantification techniques and imaging technologies.

### Materials and methods

#### Patient data

<sup>99m</sup>Tc-DMSA imaging data for pediatric patients were obtained from a combination of retrospective imaging data analysis and prospective data collection. Under an approved Institutional Review Board (IRB) protocol, data from 54 pediatric patients: 40 females and 14 males, ages ranging from 1 to 16 years old (Additional file 1) were retrospectively evaluated to extract the fraction of administered activity in the kidneys. These data were supplemented with prospective imaging in 23 (age range: 4 months to 6 years old) patients. To accommodate the special considerations in imaging pediatric patients prospectively, a data collection scheme was devised in which patients undergoing standard of care imaging were asked to consent to being imaged at one additional time point. No patient was asked to undergo more than one additional imaging time point (Fig. 1).

In the prospective study, two age groups were enrolled: less than 1 year, and between 4 to 6 years. In addition to the routine, standard-of-care, SPECT imaging, half of the subjects were imaged between 30 and 90 min, post-administration. The 2<sup>nd</sup> half were

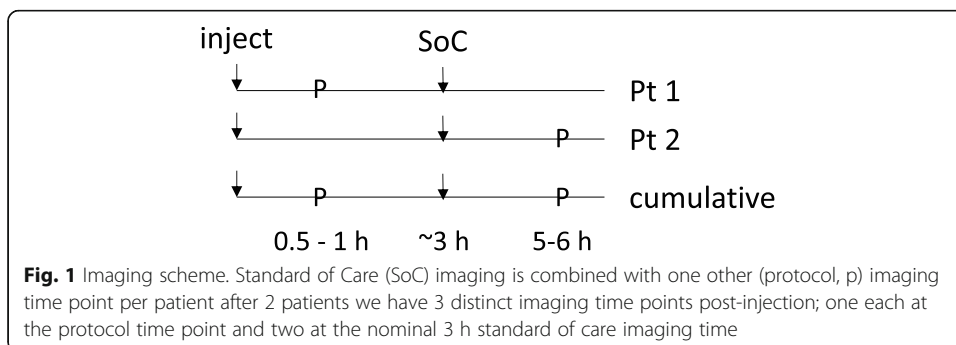


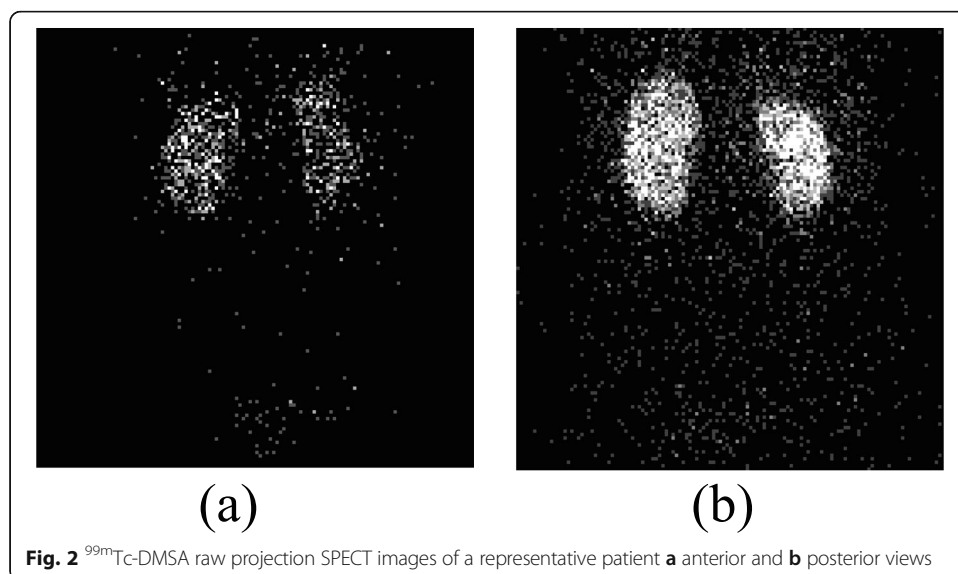
**Fig. 1** Imaging scheme. Standard of Care (SoC) imaging is combined with one other (protocol, p) imaging time point per patient after 2 patients we have 3 distinct imaging time points post-injection; one each at the protocol time point and two at the nominal 3 h standard of care imaging time

imaged at 5–6 h, post-administration. Planar imaging was acquired at these non-standard-of-care time points and at the standard of care time point either immediately before or after the clinically indicated SPECT. In general, we did not find renal pathology (focal defects) to have a significant impact on overall kidney uptake; cases in which it did were excluded from our analysis.

#### Activity quantification—retrospective study

Retrospective imaging analysis was performed by extracting single-photon emission computed tomography (SPECT) images from the Boston Children’s Hospital (BCH) image database. These were reconstructed using attenuation, scatter, and collimator response compensation.

DMSA projections were acquired on a Siemens ECAT or Symbia SPECT scanner using low-energy ultra-high resolution (LEUHR) parallel-hole collimators, a 15% energy window, 120 projection views for each detector over 360° using a body contouring orbit, and a duration of 8 s at each projection view. To enable attenuation compensation, we generated attenuation maps by reconstructing data from a scatter window (108–129 keV) using an initial attenuation map defined by the orbit of the camera [16]. The attenuation maps were then collapsed axially over a slice range spanning the kidneys. Thresholding was then used to define the body contour. The body contours generated in this manner were verified as being visually reasonable. The voxels inside the body contour were set to the attenuation coefficient of soft tissue at the 140 keV gamma energy of  $^{99m}\text{Tc}$ , repeated axially to span the kidney region, and used in the reconstruction. The activity distributions were reconstructed using the ordered subset expectation maximization (OS-EM) [17] algorithm with compensation for attenuation, the distance-dependent geometric collimator-detector response function, and scatter [18–20]. A total of 5 iterations with 16 subsets per iteration were used. Fig. 2a and b show the raw projection data for one of the patients, anterior and posterior views, respectively. Figure 3 shows the generated attenuation map and the reconstructed SPECT



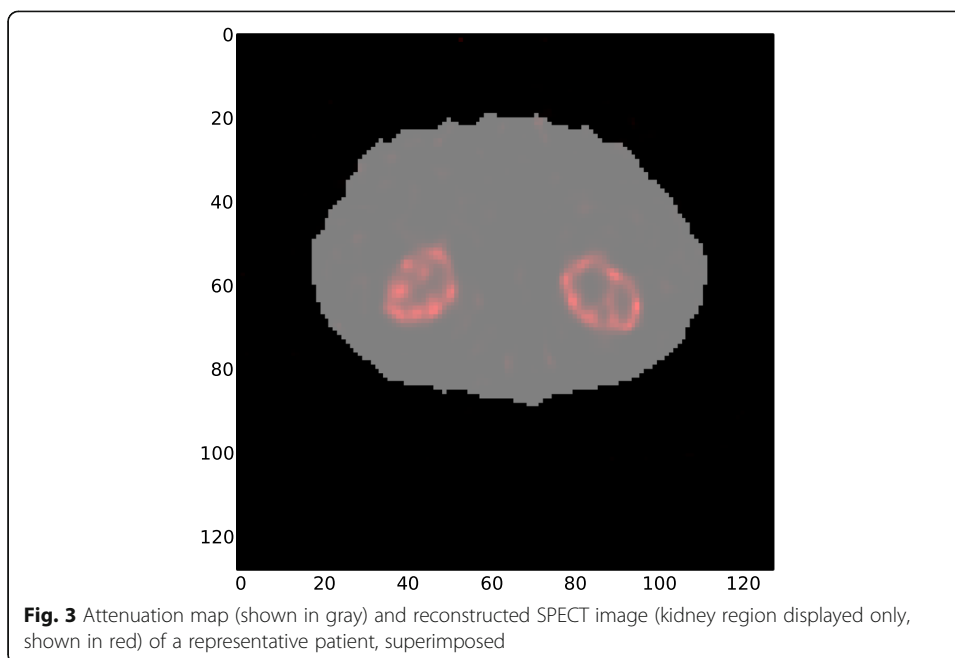


image (superimposed) for a representative patient SPECT study. A threshold was applied to the reconstructed images to define the kidneys and to obtain the sum of the reconstructed voxel value within the kidneys. This value was converted to activity using the measured sensitivity of the collimator–detector system and the total duration of the acquisition.

The camera system's sensitivity was calculated using a phantom prepared by filling a 40-ml culture flask with 39.96 MBq of  $^{99m}\text{Tc}$  and enough water to cover the  $3.5 \times 6.5 \text{ cm}^2$  area of a flat cell culture medium flask but not enough to cause significant attenuation. The phantom was placed on the collimator surface and a 1-min image was acquired with a 15% energy window, similar to that used clinically. The acquisition was repeated for the second detector. The activity was decay corrected to the time of the acquisition and the sensitivity of each detector in counts per minute per MBq (CPM/MBq) was determined.

The percent of injected activity (%IA) presented in the kidneys at the imaging time was calculated from the quantified data. This retrospectively collected patient data set provided fractional activity uptake in the kidneys at the imaging time, approximately 3 h post-injection. Since the field of view (FOV) in the provided SPECT images was limited to the abdominal area displaying the kidneys and since the uptake in the nearest organs of interest (liver and spleen) was low and at background level, it was not possible to quantify and extract activity uptake in the liver and spleen from this data set. Therefore, this data set provided a single activity time point for the kidneys only.

#### Activity quantification—prospective study

For the 23 patients enrolled prospectively, renal SPECT was performed at 2–3 h post-injection (p.i.) of  $^{99m}\text{Tc}$ -DMSA. A planar image was also acquired at the clinical time point for all patients immediately after the SPECT acquisition. A 2<sup>nd</sup> planar image was

acquired between 15 and 90 min p.i. (13 patients, early group), or at 4–6 h p.i. (10 patients, delayed imaging group). SPECT images were reconstructed iteratively with attenuation, scatter, and collimator–detector response compensations. As CT images were not available, an attenuation map was generated from the reconstructed scatter window data. The renal activity was measured in the SPECT images and the %IA was calculated. Renal activity was also measured in both planar images and corrected for scatter, background and attenuation. Kidney activity from SPECT was used in conjunction with the planar image at the clinical time point to provide a factor to quantify the activity in the 2<sup>nd</sup> planar image. The extracted PK data were used in the PK model development and validation.

### Mathematical fitting

Although the ICRP PK model as well as several authors have provided fitted expression for <sup>99m</sup>Tc-DMSA PK for organs other than the kidneys, we found the uptake in these other organs to be too low for reliable quantification. Instead, we have fitted the general kinetic expression specified by the ICRP [4] to the kidney time–activity data obtained from pediatric patients, defined as:

$$\frac{A_s(t)}{A_0} = F_s \sum_i a_i \cdot \exp\left(-\frac{\ln(2)}{T_i} \cdot t\right); \quad (1)$$

where,

$A_s(t)$  — source (S) tissue activity as a function of time,

$A_0$  — administered activity,

$F_S$  — fraction of  $A_0$  in S at back-extrapolated time zero,

$a_i$  — fraction of  $F_S$  obeying exponential kinetics with  $T_i$ , and

$T_i$  — half-life for exponential kinetic component,  $i$ .

Equation 1 gives the fraction of injected activity in an organ at each point in time; the equation assumes that there is immediate uptake in the organ (i.e. parameters are estimated assuming no uptake phase). The parameter,  $F_S$ , as defined by the ICRP, in publication 53 is the fractional distribution to organ or tissue S (i.e. the fraction of the administered activity that would arrive in source organ or tissue S overall time if there were no radioactive decay);  $a_i$  is the fraction of  $F_S$  eliminated with a biological half-time  $T_i$ .

The SAAM II software package (The Epsilon Group, Charlottesville, VA, USA) was used to obtain parameters values and their standard deviation by fitting Eq. 1 to the data [21]. The data were binned into 10-min increments for fitting (Table 1).

### Statistical evaluation of age, weight, and sex differences

Quantile regression analysis on the 50th percentile (median regression) was used to assess the independent association between DMSA kidney activity fraction and age, weight, and sex. Median regression was used to account for potential non-normality of the outcome. Univariate and multivariable adjusted median regression analyses were performed with results presented as coefficients with corresponding 95% confidence intervals and  $P$  values. Statistical analysis was performed using Stata (version 16.0, Stata-Corp LLC, College Station, TX, USA).

**Table 1** Binned kidney activity fraction data used to fit expression 1 (from retrospective data analysis)

Time interval (h)	No. of patients	Time (h)	Average kidney activity fraction	St. dev. in kidney act. fraction	Coeff. of variation in kidney act. fraction (%)
0.17–0.32	1	0.24	0.096	-	-
0.50–0.65	3	0.58	0.167	0.014	8.4
0.67–0.82	4	0.74	0.215	0.063	29.2
0.83–0.98	1	0.91	0.300	-	-
1.17–1.32	2	1.24	0.193	0.071	37.1
1.67–1.82	1	1.74	0.434	-	-
1.83–1.98	1	1.91	0.321	-	-
2.17–2.32	2	2.24	0.283	0.002	0.8
2.33–2.48	2	2.41	0.317	0.027	8.5
2.50–2.65	9	2.58	0.335	0.028	8.4
2.67–2.82	14	2.74	0.320	0.066	20.7
2.83–2.98	17	2.91	0.294	0.065	22.3
3.00–3.15	22	3.08	0.326	0.065	20.0
3.17–3.32	5	3.24	0.283	0.086	30.3
3.33–3.48	2	3.41	0.336	0.046	13.7
3.50–3.65	1	3.58	0.353	-	-
3.67–3.82	1	3.74	0.244	-	-
3.83–3.98	1	3.91	0.433	-	-
4.00–4.15	1	4.08	0.341	-	-
4.17–4.32	3	4.24	0.366	0.058	15.7
4.33–4.48	1	4.41	0.344	-	-
4.67–4.82	2	4.74	0.395	-	-
5.67–5.82	1	5.74	0.474	-	-

## Results

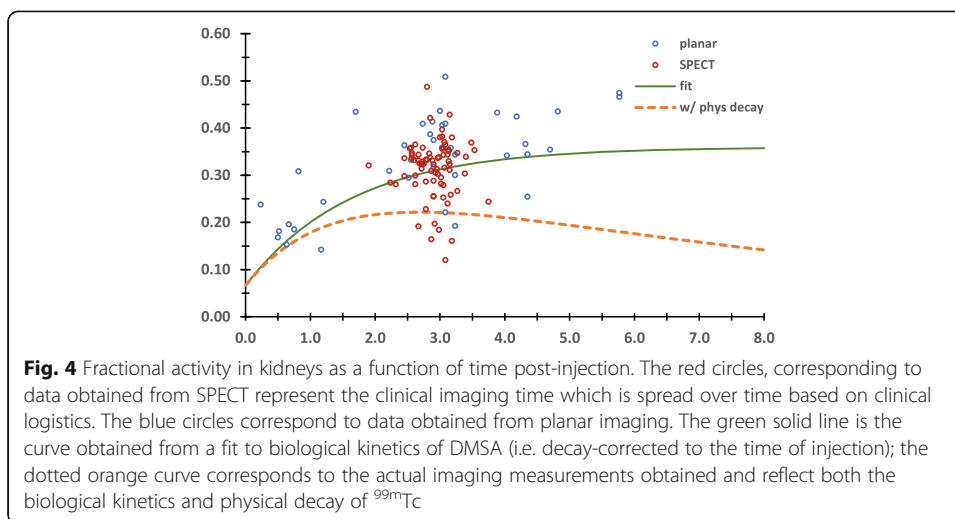
The fractional kidney activity, calculated as the total activity measured in the kidneys divided by injected activity for the combined retrospective and prospective patients, was plotted according to the elapsed time between injection and imaging (Fig. 4).

Across the entire data set, the elapsed time ranged from 0.17 to 5.82 h. The clinically indicated SPECT was acquired as early as 1.9 to as late as 3.75 h after administration. A fit of Eq. 1 to the data shown on Fig. 4 gave an  $F_S = 0.3 \pm 0.04$ ,  $a_1 = -1.0$ ,  $T_1 = 1.1 \pm 0.4$ ,  $a_2 = 1.2 \pm 0.9$ ,  $T_2 \rightarrow \infty$ ; a unique fit to the data was obtained only after  $a_1$  was fixed to  $-1.0$  and  $T_2$  was set to a very large number relative to the time scale of the data. Rearranging Eq. 1 using these parameters, the following equation is obtained:

$$\frac{A_s(t)}{A_0} = 0.3 \left( 1.2 - \exp\left(\frac{-\ln(2)}{1.1 \text{ h}} \cdot t\right) \right) \quad (2)$$

Multiplying the right-hand side of Eq. 2 by the physical decay term for  $^{99\text{m}}\text{Tc}$  (i.e.  $\exp\left(\frac{-\ln(2)}{6.0 \text{ h}} \cdot t\right)$ ) and integrating from zero to infinity gives  $\frac{\tilde{A}_s}{A_0} = 2.7 \pm 0.4 \text{ h}$ .

Figure 5 shows the renal activity fraction at the clinical imaging time as a function of patient weight, height, age, and sex.



The data set used in statistical analysis are summarized on Table 2. Tables 3 and 4 list the results of univariate and multivariate analysis, respectively. Weight and sex were found as significantly associated with kidney activity fraction. Using a multivariable median regression strategy, sex was an independent predictor of kidney activity fraction (coefficient for female sex (0.064) higher than males; 95% CI: 0.032–0.097;  $P < 0.001$ ).

## Discussion

The biokinetics of  $^{99m}\text{Tc}$ -DMSA are well documented for adult patients [4, 9] but not for pediatric patients. The age-specific absorbed and effective dose values listed in ICRP 128 [9] are adjusted for differences in anatomy but the biokinetic models used in these calculations are derived from adult data.

As part of an overall effort to revisit and further optimize the activity administered to pediatric patients for nuclear medicine imaging, we have recently examined the impact of a number of variables on image quality and the relationship between imaging quality, administered activity, pediatric patient absorbed dose and the risk of potential detrimental effects for  $^{99m}\text{Tc}$ -DMSA [10–15, 22–24].

In this work, we collected pharmacokinetic data for pediatric patients by combining quantitative SPECT and planar imaging. Planar imaging was quantified by calibrating the activity values obtained to those obtained from SPECT collected during the same imaging session (i.e. based on hybrid imaging technique [25]). Over the time points measured, we found that the count rate in the liver and spleen was too low to accurately assess kinetics in these tissues. We, therefore, focused on the kidneys and adopted the sum of exponential formulations used by the ICRP to parameterize the measurements. We also examined the fractional uptake at the clinical imaging time. Over the age range examined, we did not find a significant difference in the renal fractional uptake at the time of imaging, but we did find that the uptake in female patients was significantly higher than in male patients. We also found that a fit of the ICRP expression to our data gave different fitted parameter values. The plateau phase in fractional kidney uptake occurs at a fractional uptake value closer to 0.3 than the 0.5 reported by the ICRP. The data also suggest a longer time interval before the plateau is reached (solid green curve of Fig. 4). The dotted orange curve of Fig. 4 (which incorporates physical

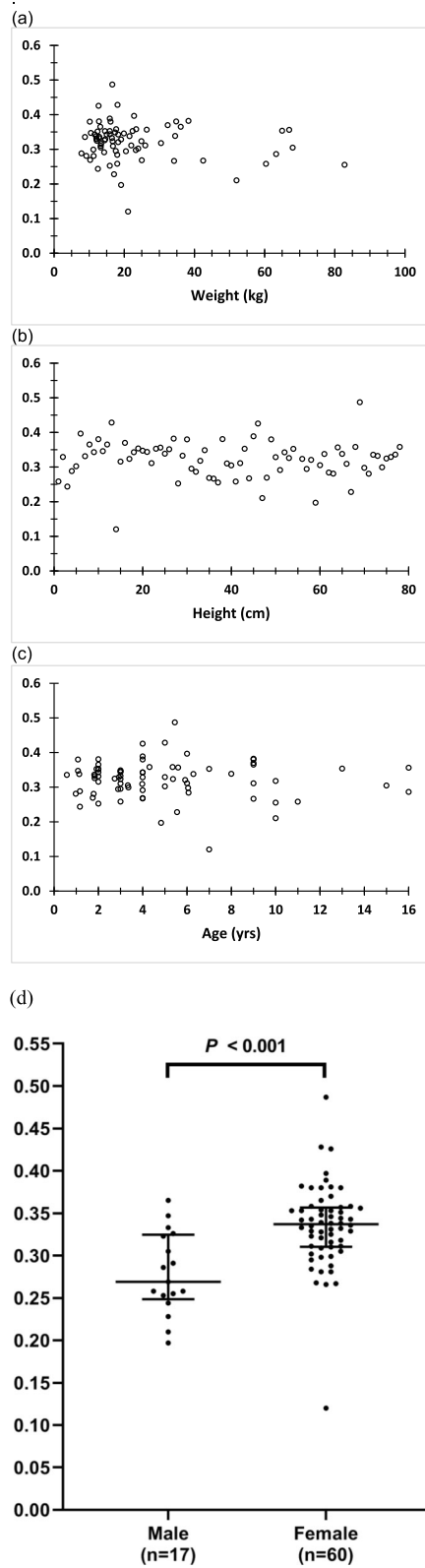


**Fig. 5** Kidney activity fraction at the clinical imaging time, approximately 3 h post DMSA administration. Data points shown are from quantitative SPECT imaging versus patient **a** weight, **b** height, **c** age and **d** gender (middle lines represent medians (50th percentile) and the interquartile ranges (25th–75th percentiles; top and bottom lines))



**Table 2** Summary of data evaluated by regression analysis

Variable	n (%) or median (interquartile range)
<i>N</i>	77
Age (years)	4 (2, 6)
Age category	
0 to < 3 years	24 (31.2%)
3 to < 7 years	36 (46.8%)
7 to < 13 years	13 (16.9%)
≥ 13 years	4 (5.2%)
Weight (kg)	17.4 (13.2, 24)
Sex	
Male	17 (22.1%)
Female	60 (77.9%)
Kidney activity fraction	0.33 (0.29, 0.35)

decay of <sup>99m</sup>Tc) suggests that the clinical imaging time reflects an appropriate balance between biological uptake of the agent in the kidneys and physical decay of <sup>99m</sup>Tc.

Although the imaging data were obtained from patients suspected of kidney pathology in the majority of cases, the overall kinetics were not affected by pathology. With accurate attenuation correction, SPECT quantification is typically within 5% [25]. Since we chose not to acquire CT to avoid unnecessary patient exposure, we used images generated from events collected in a scatter window to define the outer body contours for attenuation correction; this could introduce a 10-to-15% uncertainty. Based on this, we conclude that the 20-to-30% variation seen in kidney uptake at 3 h post DMSA administration (i.e. the “clinical” imaging time) most likely reflects patient-to-patient variability in DMSA uptake. Since the clinical diagnosis is primarily based upon identifying regions of diminished uptake, such overall variability does not impact the diagnostic imaging task but it does reflect that variability in kidney-absorbed dose for a pediatric patient population.

**Table 3** Univariate median regression analysis of kidney activity fraction

Variable	Coefficient	95% CI	P value
Age (per year)	− 0.002	(− 0.006, 0.002)	0.254
Age category			
0 to < 3 years	Reference	.	.
3 to < 7 years	− 0.004	(− 0.035, 0.027)	0.795
7 to < 13 years	− 0.014	(− 0.054, 0.026)	0.487
≥ 13 years	− 0.027	(− 0.09, 0.036)	0.393
Weight (per 5 kg)	− 0.004	(− 0.008, 0.001)	0.087
Sex			
Male	Reference	.	.
Female	0.067	(0.038, 0.096)	< 0.001*

Quantile regression on the median (median regression) was used to determine the univariate associations between each variable and kidney activity fraction.

\*Statistically significant

**Table 4** Multivariable median regression analysis of kidney activity fraction

Covariate	Adjusted Coefficient	95% CI	P value
Age (per year)	0.003	(− 0.004, 0.011)	0.4
Weight (per 5 kg)	− 0.003	(− 0.012, 0.006)	0.532
<b>Sex</b>			
Male	Reference	.	.
Female	0.064	(0.032, 0.097)	< 0.001*

Multivariable quantile regression on the median (median regression) was used to determine the independent associations between each variable and kidney activity fraction.

\*Statistically significant

Evans et al. [26], presented <sup>99m</sup>Tc-DMSA biokinetic data from children of different ages and degrees of renal dysfunction. Using planar imaging, Evans et al. obtained biokinetic information for liver and spleen where they measured maximum uptake values that were 10-fold less than found for the kidneys.

Table 5 compares the fitted parameters obtained in the current study with those reported by Evans et al. and those listed in ICRP publications 53 and 128. The last column of this table lists the time-integrated activity coefficient (TIAC), formerly called the residence time. The value obtained for pediatric patients obtained in this work is 27% lower than that reported by the ICRP; the value calculated from data reported by Evans is 19% lower but the standard deviation of the result is 100% of the value largely due to the very high standard deviation associated with  $T_2$ .

Longitudinal imaging data in pediatric patients for imaging agents including <sup>99m</sup>Tc-DMSA have been severely lacking. The results presented herein suggest that the pediatric TIAC to kidney is lower than that reported by the ICRP and that, therefore, the absorbed dose and effective doses may also be lower. Over the age range examined, no age dependency in kidney fractional uptake was observed. A significantly ( $P < 0.001$ ) higher fractional kidney uptake in female ( $0.33 \pm 0.05$ ) relative to male ( $0.38 \pm 0.05$ ) patients was also observed (Tables 3 and 4 and Fig. 5d). Correspondingly, the absorbed and the effective doses are expected to be higher for female pediatric patients than for males. Renal maturation appears to occur within the first year ([27, 28] Chapter 12). The data used for the ICRP DMSA model were collected in the mid-1970’s. Since no age dependency in uptake fraction at the time of imaging was observed, the difference between kinetic parameter values obtained in the current study and those reported in ICRP 53 and 128 may reflect an improvement in imaging quantification rather than a difference between pediatric patients and adults. A re-examination of adult DMSA kinetics may, therefore, be merited.

**Conclusions**

Currently available pediatric dose estimates for <sup>99m</sup>Tc-DMSA use pediatric  $S$  values with PK data derived from adults. We have examined whether the current reference (ICRP 53 [4])

**Table 5** Comparison of Tc-99m DMSA model parameters ( $\pm$  standard deviations) for the kidneys

Parameter	$F_S$	$T_1$ (h)	$T_2$ (h)	$a_1$	$a_2$	$\tilde{A}_s / A_0$ (h)
ICRP 53	0.5	1.0	$\infty$	− 1	1	3.71
Evans et al.	$0.4 \pm 0.05$	$1.0 \pm 0.2$	$7 \pm 6$	− 1	1	$3 \pm 3$
Current study	$0.3 \pm 0.04$	$1.1 \pm 0.4$	$\infty$	− 1	$1.2 \pm 0.9$	$2.7 \pm 0.4$

DMSA PK model is consistent with model parameters obtained by  $^{99m}\text{Tc}$ -DMSA imaging measurements in children. Pharmacokinetics obtained in this study yield a 27% lower time-integrated activity coefficient in pediatric patients than in adults. Female pediatric patients had a 17% higher fractional kidney uptake at the clinical imaging time than males. These results suggest that a separate pediatric DMSA model is necessary to properly account for DMSA PK differences between children and adults. Furthermore, since adult DMSA kinetics were collected in the mid-70's, a re-examination of adult DMSA kinetics is merited.

### Supplementary Information

The online version contains supplementary material available at <https://doi.org/10.1186/s40658-021-00401-7>.

**Additional file 1: Table 1.** Patients' Characteristics Data.

### Acknowledgements

The authors acknowledge the support provided by National Institutes of Health grant No. R01EB013558.

### Authors' contributions

DP and MG wrote the manuscript and were involved in data collection and analysis; YL, JLB, SO, KK, ABG, BSS, XC, and DZ were involved in either data collection, analysis or patient protocol support for patient enrollment; they also reviewed the manuscript. FHF, STT, WEB, ECF, and GS guided and supervised the work and reviewed the manuscript. FHF and STT also recruited patients for the study. The author(s) read and approved the final manuscript.

### Funding

This study was funded by the National Institutes of Health grant No. R01EB013558.

### Availability of data and materials

Data and materials related to this manuscript will be made available upon request.

### Declarations

#### Ethics approval and consent to participate

All procedures performed in studies involving human participants were reviewed and approved by the Boston Children's Hospital Institutional Review Board (IRB); they are in accordance with ethical standards set forth in the 1964 Helsinki declaration and its later amendments. All study participants gave their informed consent to participate in the study.

#### Consent for publication

All authors have reviewed this manuscript and consent to its publication.

#### Competing interests

The authors have no competing interests.

#### Author details

<sup>1</sup>The Russell H. Morgan Department of Radiology and Radiological Science, Johns Hopkins University, School of Medicine, Baltimore, MD, USA. <sup>2</sup>J. Crayton Pruitt Family Department of Biomedical Engineering, University of Florida, Gainesville, FL, USA. <sup>3</sup>Department of Radiology, Faculty of Medicine, Chulalongkorn University and King Chulalongkorn Memorial Hospital, Thai Red Cross Society, Bangkok, Thailand. <sup>4</sup>Division of Nuclear Medicine and Molecular Imaging, Boston Children's Hospital, Harvard Medical School, Boston, MA, USA. <sup>5</sup>Departments of Anesthesiology and Surgery, Boston Children's Hospital, Harvard Medical School, Boston, MA, USA. <sup>6</sup>Division of Nuclear Medicine and Molecular imaging, Department of Radiology, Brigham and Women's Hospital, Harvard Medical School, Boston, MA, USA.

Received: 5 October 2020 Accepted: 5 July 2021

Published online: 20 July 2021

### References

1. Gelfand MJ, Parisi MT, Treves ST. Pediatric radiopharmaceutical administered doses: 2010 North American consensus guidelines. *J Nucl Med.* 2011;52(2):318–22. <https://doi.org/10.2967/jnumed.110.084327>.
2. Fahey FH, et al. Effects of image gently and the North American guidelines: administered activities in children at 13 North American pediatric hospitals. *J Nucl Med.* 2015: p. jnumed. 114.148767. <https://doi.org/10.2967/jnumed.114.148767>.
3. Treves ST, Gelfand MJ, Fahey FH, Parisi MT. 2016 Update of the North American consensus guidelines for pediatric administered radiopharmaceutical activities. *J Nucl Med.* 2016;57(12):15N–8N.
4. ICRP. Publication 53: radiation dose to patients from radiopharmaceuticals, 53. *Ann ICRP.* 1988;18:1–4.
5. Arnold RW, Subramanian G, McAfee J, Blair RJ, Thomas FD. Comparison of Tc-99m complexes for renal imaging. *J Nucl Med.* 1975;16(5):357–67.

6. Elliott AT, et al. Dosimetry of current radiopharmaceuticals used in renal investigation. In Proceedings Radiopharmaceutical Dosimetry Symposium. Oak Ridge Tennessee. 1976:293–304).
7. Enlander D, Weber PM, dos Remedios LV. Renal cortical imaging in 35 patients: superior quality with 99mTc-DMSA. *J Nucl Med.* 1974;15(9):743–9.
8. Handmaker H, Young BW, Lowenstein JM. Clinical experience with Tc-99m-DMSA (dimercaptosuccinic acid), a new renal-imaging agent. *J Nucl Med.* 1975;16(1):28–32.
9. Mattsson S, et al. Radiation dose to patients from radiopharmaceuticals: a compendium of current information related to frequently used substances (vol 44, pg 7, 2015). *Ann ICRP.* 2019;48(1):96.
10. Sgouros G, Frey EC, Bolch WE, Wayson MB, Abadia AF, Treves ST. An approach for balancing diagnostic image quality with cancer risk: application to pediatric diagnostic imaging of 99mTc-dimercaptosuccinic acid. *J Nucl Med.* 2011;52(12):1923–9. <https://doi.org/10.2967/jnumed.111.092221>.
11. O'Reilly SE, Plyku D, Sgouros G, Fahey FH, Ted Treves S, Frey EC, et al. A risk index for pediatric patients undergoing diagnostic imaging with 99mTc-dimercaptosuccinic acid that accounts for body habitus. *Phys Med Biol.* 2016;61(6):2319–32. <https://doi.org/10.1088/0031-9155/61/6/2319>.
12. Li Y, et al. Patient girth is better than weight for selecting administered activity in renal pediatric imaging. *J Nucl Med.* 2019;60(supplement 1):154.
13. Li Y, et al. Limitation of weight-based pediatric dosing guidelines in 99mTc-DMSA renal SPECT. *J Nucl Med.* 2018;59(supplement 1):309.
14. Fahey FH, Goodkind AB, Plyku D, Khamwan K, O'Reilly SE, Cao X, et al. Dose estimation in pediatric nuclear medicine. *Semin Nucl Med.* 2017;47(2):118–25. <https://doi.org/10.1053/j.semnuclmed.2016.10.006>.
15. Li Y, O'Reilly S, Plyku D, Treves ST, Fahey F, du Y, et al. Current pediatric administered activity guidelines for (99m) Tc-DMSA SPECT based on patient weight do not provide the same task-based image quality. *Med Phys.* 2019;46(11):4847–56. <https://doi.org/10.1002/mp.13787>.
16. Pan TS, et al. Segmentation of the body and lungs from Compton scatter and photopeak window data in SPECT: a Monte Carlo investigation (vol 15, pg 13, 1996). *IEEE Trans Med Imaging.* 1996;15(3):394–6.
17. Hudson HM, Larkin RS. Accelerated image reconstruction using ordered subsets of projection data. *IEEE Trans Med Imaging.* 1994;13(4):601–9. <https://doi.org/10.1109/42.363108>.
18. Frey EC, Tsui BMW, Kadrmaz DJ. A new method for modeling the spatially-variant, object-dependent scatter response function in SPECT. In: 1996 IEEE Nuclear Science Symposium. Conference Record. Anaheim, San Francisco: IEEE; 1996.
19. Kadrmaz DJ, Frey EC, Karimi SS, Tsui BMW. Fast implementations of reconstruction-based scatter compensation in fully 3D SPECT image reconstruction. *Phys Med Biol.* 1998;43(4):857–73. <https://doi.org/10.1088/0031-9155/43/4/014>.
20. He B, du Y, Song X, Segars WP, Frey EC. A Monte Carlo and physical phantom evaluation of quantitative In-111 SPECT. *Phys Med Biol.* 2005;50(17):4169–85. <https://doi.org/10.1088/0031-9155/50/17/018>.
21. Barrett PHR, Bell BM, Cobelli C, Golde H, Schumitzky A, Vicini P, et al. SAAM II: simulation, analysis, and modeling software for tracer and pharmacokinetic studies. *Metabolism.* 1998;47(4):484–92. [https://doi.org/10.1016/S0026-0495\(98\)90064-6](https://doi.org/10.1016/S0026-0495(98)90064-6).
22. Wayson M, Lee C, Sgouros G, Treves ST, Frey E, Bolch WE. Internal photon and electron dosimetry of the newborn patient—a hybrid computational phantom study. *Phys Med Biol.* 2012;57(5):1433–57. <https://doi.org/10.1088/0031-9155/57/5/1433>.
23. Khamwan K, Plyku D, O'Reilly SE, Goodkind A, Cao X, Fahey FH, et al. Pharmacokinetic modeling of F-18 fluorodeoxyglucose (FDG) for premature infants, and newborns through 5-year-olds. *EJNMMI Res.* 2016;6(1):28. <https://doi.org/10.1186/s13550-016-0179-6>.
24. Brown J, et al. Pediatric S-values for a multiregional brain model. *J Nucl Med.* 2019;60(supplement 1):1631.
25. He B, du Y, Segars WP, Wahl RL, Sgouros G, Jacene H, et al. Evaluation of quantitative imaging methods for organ activity and residence time estimation using a population of phantoms having realistic variations in anatomy and uptake. *Med Phys.* 2009;36(2):612–9. <https://doi.org/10.1118/1.3063156>.
26. Evans K, Lythgoe MF, Anderson PJ, Smith T, Gordon I. Biokinetic behavior of technetium-99m-DMSA in children. *J Nucl Med.* 1996;37(8):1331–5.
27. Lythgoe MF, Gordon I, Anderson PJ. Effect of renal maturation on the clearance of Tc-99m mercaptoacetyltriglycine. *Eur J Nucl Med.* 1994;21(12):1333–7. <https://doi.org/10.1007/BF02426698>.
28. Treves ST, Packard AB, Grant FD. Kidneys, Chapter 12. In: *Pediatric Nuclear Medicine and Molecular Imaging*. 4th ed. New York: Springer; 2014. <https://doi.org/10.1007/978-1-4614-9551-2>.

## Publisher's Note

Springer Nature remains neutral with regard to jurisdictional claims in published maps and institutional affiliations.